GEOPHYSICAL RESEARCH LETTERS, VOL. 25, NO. 12, PAGES 2069-2072, JUNE 15, 1998

FAST observations of electron distributions within AKR source regions.

G.T. Delory, R.E. Ergun, C.W. Carlson, L. Muschietti, C.C. Chaston, W. Peria, and J.P. McFadden

Space Sciences Laboratory, University of California, Berkeley

R. Strangeway

Institute of Geophysical and Planetary Physics, University of California, Los Angeles

Abstract. Observations of high-time resolution 3-D electron distributions within the source regions of Auroral Kilometric Radiation (AKR) are reported. In general, the electron data display a broad plateau over a wide range of pitch angles indicating that these distributions have been rapidly stabilized by AKR wave growth. The source of the electron instability appears to come from several features in the distribution, including an isotropic beam feature and its mirroring components, occasional electrons in the "trapped" region, as well as steep gradients present in the atmospheric loss cone. Taken together these features may provide a nearly continuous region of $\partial f/\partial v_\perp$ which could contribute to the relativistic cyclotron maser instability. Computer simulations of the evolution of the electron distribution which assume plasma conditions similar to the parameters measured by FAST show similar results to the observed electron distributions. The FAST observations also show that relativistic corrections to the AKR dispersion relation may enable a small $k_\parallel$ mode with a resonance condition that is able to take maximum advantage of the initial instability in the mono-energetic electron distributions within the auroral acceleration regions.

Introduction

The FAST satellite has made numerous high-time resolution measurements of Auroral Kilometric Radiation (AKR) and associated 3-D electron distributions. Many of these measurements have occurred while we believe the satellite was inside the AKR source region, within the auroral acceleration potential where we find inverted-V electrons, upgoing collimated ion beams and a significant density depletion of the cold background electron plasma (see the paper by *Ergun et al.*, [1998], this issue, for a general description of AKR observations made by FAST.) Within the AKR source regions, the energetic electron distributions appear to be plateaued over a wide range of pitch angles. We interpret this plateau as the result of diffusion in velocity space due to AKR wave growth. In general, most of the distributions we measure are plateaued in a region about $v_\parallel = 0$, with a loss cone present in the upgoing component and a slight positive slope in the field-aligned downgoing region due to the primary inverted-V electrons.

The earliest successful theories for describing an instability mechanism responsible for the generation of AKR dealt with a relativistic Doppler-shifted cyclotron maser effect in which the electron gyroresonance condition was modified by a relativistic term:

Paper number 98GL00705.
0094-8534/98/98GL-00705-$05.00

$$\omega - (n\Omega_e)/\gamma - k_\parallel v_\parallel = 0 \quad (1)$$

This resonance condition results in a series of ellipses in velocity space for various values of $k_\parallel$ and the local plasma parameters (*Omidi et al.*, 1984.) The central issue in most of the cyclotron resonance work has been the identification of sources of free energy in the electron distribution where a certain set of resonant ellipses given by Equation (1) could sample a sufficient amount of positive gradient in the distribution for effective wave growth. The work by *Wu and Lee* [1979] is perhaps best known for calculating the growth rate for this instability by assuming that favorable conditions for wave growth could be found in the loss-cone region of the distribution, where frequently $\partial f/\partial v_\perp > 0$. Observations from the S3-3 satellite and more recently from the Viking spacecraft near the AKR source regions have shown that this positive slope does exist in a typical inverted-V electron distribution [*Mizera & Fennell*, 1977; *Ungstrup et al.*, 1990]. Moreover, this emission mechanism could also account for the fact that the polarization for AKR appeared to be primarily in the *R-X* mode (*Shawhan & Gurnett*, 1982.) Later work has attempted to identify other features in the electron distribution which may contain free energy, such as in a trapped electron population (*Louarn et al.*, 1990).

The high time-resolution results from FAST suggest that the region of $\partial f/\partial v_\perp > 0$ occurs over a wide range of pitch angles in the energetic electron distribution. Nearly all of the examples presented show a broad, flat plateau in the distribution extending out from ~30° away from the field-aligned direction all the way back to the loss cone, with an occasional remnant of a positive slope in the parallel direction due to the primary inverted-V electrons. This distribution is assumed to be a result of the wave-particle diffusion of an incident mono-energetic beam which is mirroring in the increasing geomagnetic field, creating a strong $\partial f/\partial v_\perp$ which may extend from the field-aligned direction toward regions near 90° pitch angles and beyond. The rapid stabilization of this type of distribution has been studied using a particle-in-cell, electromagnetic code in the work by *Winglee and Pritchett* [1986], *Pritchett and Strangeway* [1985], and *Pritchett and Winglee* [1989]. These simulations assume several conditions which are applicable to the FAST data: the cold background density is small compared to the energetic electron density and relativistic corrections to the AKR dispersion relation allow for emissions with negligible $k_\parallel$ and with frequencies below the non-relativistic, cold-plasma electron cyclotron frequency Ω_e. The resulting electron distributions from these simulations show a broad plateau very similar to what is observed in the FAST electron distributions during passes throughout the AKR source regions. In addition, it is shown that by assuming a negligible $k_\parallel$, which is allowed when relativistic effects are taken into account, the AKR resonance condition can take maximum advan-

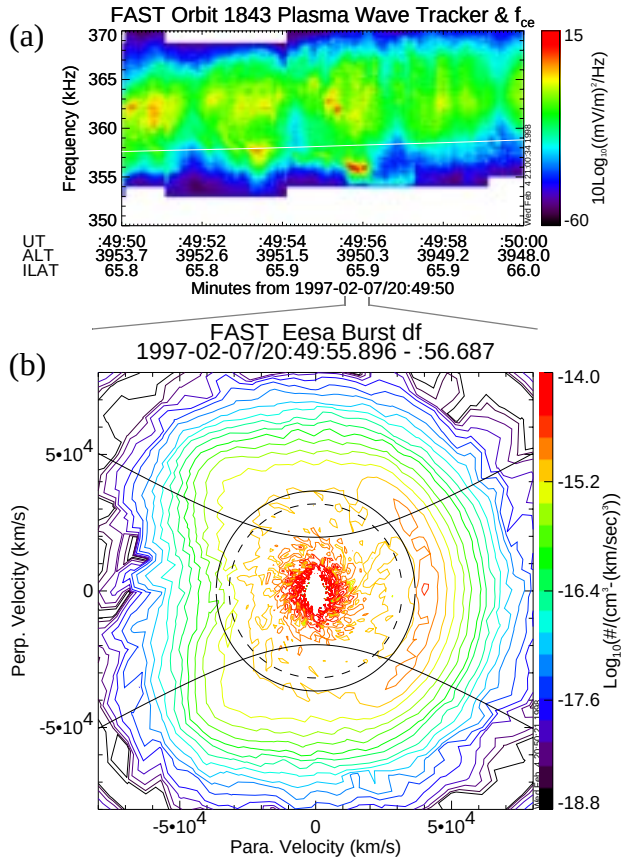

Figure 1. (a) Plasma Wave Tracker data and (b) electron contour plot for orbit 1843. The solid lines represent boundaries for adiabatic motion of electrons (see *Chiu and Schulz* [1978]), while the dotted inner circle shows the resonance condition with $k_{\|} = 0$ in Equation (1) for the AKR burst near ~20:49:56 UT.

tage of the initial instability created by the incident mirroring inverted-V electrons. These conclusions are similar to those reached by *Menietti et al.*, [1993] who examined electron data from the DE-1 spacecraft during AKR emissions.

FAST Observations

Detailed AKR wave spectra and electron distribution contour plots in ($v_{\|}$, $v_{\perp}$) space are shown from two FAST crossings of the AKR source regions on orbits 1843 and 1907. An example of an AKR source crossing by FAST is shown in Figure 1 for orbit 1843. The Plasma Wave Tracker instrument is capable of 16 msec time resolution and 100 Hz frequency resolution as it samples a 16 kHz bandwidth centered on Ω_e, and shows emissions generated at just above and below Ω_e in Figure 1(a). The white line on the tracker spectrogram shows the locally measured Ω_e. An electron contour plot is shown in Figure 1(b), which represents an average of 10 80 msec analyzer sweeps while the FAST satellite was in "burst" mode, centered on a time near ~49:56 where an AKR burst below Ω_e briefly appears. In order to understand the various possible regions of free energy in the distribution it is useful to divide different regions of the contour plot in terms of the various electron populations that are present. Superimposed on the electron contour plot are solid black boundaries defining regions of magnetospheric, ionospheric, and trapped electron populations as described by *Chiu and Schulz* [1978]. The nearly circular ellipse defines a boundary for the accelerated, magnetospheric electrons; these electrons cannot occupy regions of the distribution below this velocity unless scattered there by some wave-particle or other interaction. The hyperbolas define the loss cone in the presence of a parallel potential drop. Because FAST is in the low-altitude auroral acceleration region at this time, there is a potential both above and below the spacecraft. The areas outside the hyperbola but within the ellipse define "trapped" regions; ordinarily, no electrons should occupy this part of phase space unless some form of scattering or possibly a time varying field-aligned potential has occurred. The region within the loss cone hyperbolas and the ellipse is then left to electrons of ionospheric origin. The primary, inverted-V energetic electrons are clearly visible, peaking at small pitch angles and spreading out to nearly 45° in pitch angle as the beam mirrors in the geomagnetic field. The loss cone is present in the upgoing direction. There is a broad plateau in this distribution outlined by the green/yellow contour lines which encompasses the ellipse defined by the accelerated electrons.

Figure 2(a) shows the AKR wave spectra obtained during orbit 1907 using the Plasma Wave Tracker instrument. The measurement shows intense, localized emissions just above Ω_e, with some emissions slightly below Ω_e. Figure 2(b) shows the electron contour plot obtained during a 3 second sub-interval of this source crossing during the intense burst on the inbound edge near ~58:56. There is a clear loss cone feature in the upward component, an enhancement in the electrons at 90° pitch angles with a negative gradient along $v_{\perp}$, and a mirroring, mono-energetic feature at $v_{\perp} = 0$ just above $v_{\|}$ ~ 5×10^4 km/sec. The enhanced fluxes of electrons at 90° occupy the forbidden region of the distribution; they have a strong negative

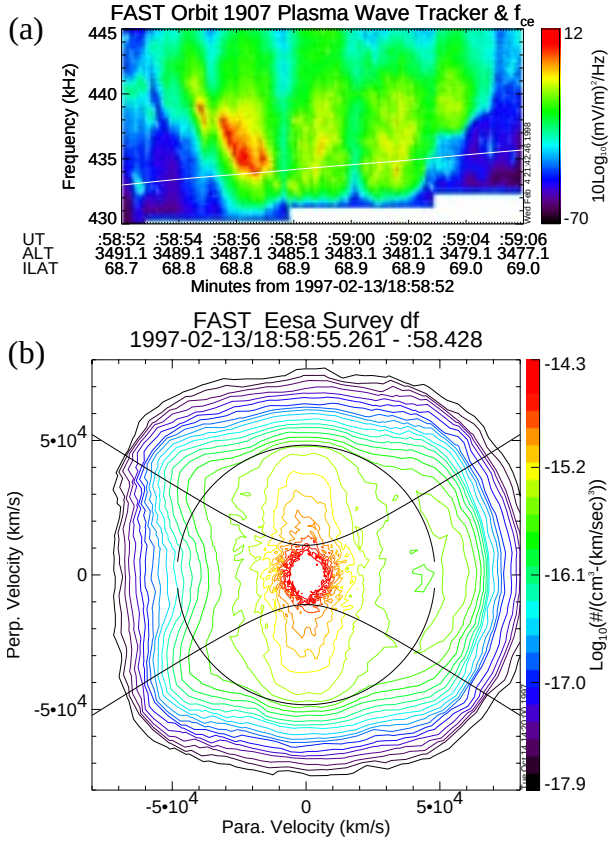

Figure 2. (a) AKR spectra measured using the Plasma Wave Tracker instrument and (b) electron contour plots obtained in this source region for FAST orbit 1907.

slope extending from very low energies (< 100 eV) out to several keV. In this example and several of the other 10 or so FAST AKR crossings examined in detail, these electrons are seen on the edges of the AKR source regions. All of these features appear to be resting on a broad plateau outlined by the green contour lines, which looks similar to the plateau in the previous example.

There are several other notable observations pertaining to the AKR source regions. While it is not apparent in the contour plots, the cold electron population n_{cold} (< 100 eV) is almost entirely depleted in the AKR source regions, with the hot electrons n_E (> 100 eV) being responsible for the bulk of the total electron density, about n_e = 1/cc for orbits 1843 and 1907. The contour plot data is contaminated by a combination of spacecraft photoelectrons (up to 60 eV) as well as secondaries emitted from the spacecraft due to the energetic electron beams, thus yielding an artificial core in the analyzer data. A detailed analysis of dispersion properties of VLF waves within these density cavities, however, supports the assertion that there is essentially no thermal electron core below 100 eV [*Ergun et al.*, 1998; *Strangeway et al.*, 1998]. Secondly, an examination of the power nulls in the AKR spectra from the Plasma Wave Tracker and 0.5 μs digital samples of the AKR waveform show that the AKR polarization is within 2-3° of **B**, indicating that these waves may have a small $k_{||}$.

Discussion

The debate over which region of the electron distribution contributes to AKR wave growth has continued since the initial suggestion by *Wu and Lee* that the free energy source of the cyclotron maser instability lies in the loss cone of the precipitating electrons. *Ungstrup et al.*, using data from the Viking satellite, have compared the loss cones both inside and outside the source regions and concluded that the loss cones within the source regions are partially filled, which they interpret as evidence that this region of the distribution provides the necessary free energy for AKR growth. *Louarn et al.* have shown that a reasonable convective growth rate can be obtained by an enhancement in the trapped electron population, assuming that a mechanism exists for placing incident magnetospheric electrons into non-adiabatic motion. Other work has examined alternative mechanisms for the production of AKR, including an upper hybrid-lower hybrid wave soliton interaction [*Pottelette et al.*, 1992].

The detailed electron measurements by FAST in the 10 or so AKR source regions examined in detail all possess one common feature; a broad plateau over a wide range of pitch angles (~0°-135°) that includes the region of the accelerated, inverted-V electrons, the trapped region, and near the loss cone. The role of the loss cone in the growth of AKR is put into question in the FAST data since we rarely observed loss cones that appear to be filled, in contrast to the Viking observations by *Ungstrup et al.* And while plateaus in the distribution are frequently seen within the trapped particle region, these plateaus clearly extend beyond that region both along $v_{||}$ and $v_{\perp}$, which may indicate that this diffusion of the electrons involves more than just trapped electrons. While *Louarn et al.* report finding electrons in the trapped region with a slight positive slope and thus could be unstable with respect to the production of AKR, such a distribution is not apparent in the FAST AKR crossings examined so far. When FAST does measure enhancements in the trapped distribution as in Figure 2(b), these electrons invariably have a strong negative gradient along $v_{\perp}$, which is not what would be expected if these electrons were once unstable and had been plateaued by AKR wave growth. Finally, to address the work on the soliton wave interactions by *Pottelette et al.*, we note that while there is frequently an intense lower hybrid line during the source crossings, upper hybrid waves have yet to be consistently associated with AKR emissions in the FAST data.

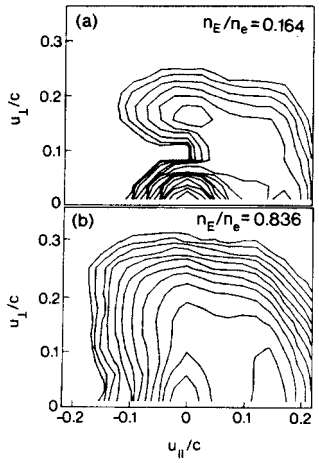

Figure 3. The results of numerical simulations shown in Figure 15 of the work by *Winglee and Pritchett* [1986]. The distribution in (a) has been stabilized by electrostatic waves; (b) shows diffusion due to AKR growth when the energetic electrons dominate the plasma.

One scenario that could produce the broad plateaus seen in the data coupled with occasional enhanced fluxes of electrons along $v_{\perp}$ has been outlined in the work by *Winglee and Pritchett*. In their model, we begin with a mono-energetic, accelerated maxwellian which has become energized by an initial acceleration region far above the FAST altitude at several R_E. As these electrons mirror to increasing pitch angles due to the gradient in the geomagnetic field, a positive slope exists for an increasingly wide range of pitch angles which may become stabilized by a variety of plasma waves. That the electrons are able to mirror to wide pitch angles by the time they reach FAST is supported not only by our observations but by the work of *Gurgiolo et al.*, [1988], who conclude that the auroral acceleration region is split into a high and a low altitude component separated by many thousands of km. At 3500 km altitude, FAST is clearly in the low altitude part of the auroral acceleration region. In the simulation by *Winglee and Pritchett*, the competition between electrostatic waves and electromagnetic emissions for the free energy in this type of distribution was characterized. For a low energetic electron density relative to the background density such that $n_E/n_e < 1$ it was found that electrostatic waves would rapidly diffuse the distribution in the parallel direction. This diffusion would tend to soften the perpendicular gradients necessary for the cyclotron maser instability, and AKR wave growth was suppressed. For $n_E/n_e > 1$ however, the situation was reversed. For an accelerated maxwellian distribution mirroring in the geomagnetic field with sufficient density compared to the cold background plasma, it was found that the maser instability beat out the parallel instability and substantial AKR wave growth could occur. These waves were produced at near perpendicular propagation close to Ω_e and yielded a broad plateau with a remnant of a parallel positive slope due to the inverted-V electrons. The resulting stabilized electron distributions from these simulations possess a remarkable resemblance to the FAST electron data. Figure 3 shows the results of the simulations

conducted by *Winglee and Pritchett*; the contours in Figure 3(a) result when the distribution has been diffused by electrostatic wave growth, which occurs when the cold electrons dominate the plasma. Figure 3(b) shows the results when the energetic electrons dominate, as in the case of FAST, resulting in a distribution stabilized by AKR growth. Note the resemblance of this result to the data in Figure 1(b). As already noted there is strong evidence in the FAST data that the cold background electrons below 100 eV are severely depleted and that the plasma is dominated by the hot electrons. In addition, *Winglee and Pritchett* found that once the AKR was generated, it could act as an electron heating mechanism for the colder ionospheric electrons, producing an enhancement of these electrons at 90° pitch angles; the beginning of this effect can be seen in Figure 3(b) for the contours of the core distribution. This could explain the enhanced electrons with a negative gradient measured by FAST at these pitch angles as seen in Figure 2(b); the examination of DE-1 data during AKR emissions led *Menietti et al.*to the same conclusion for the source of these electrons. For these simulations it was also noted that a relativistic dispersion analysis [*Strangeway*, 1985; *Strangeway*, 1986] yielded modes which could exist below the local cold-plasma Ω_e. These modes could have a $k_{||} = 0$ and grow at a 90° propagation angle; thus the resonant ellipse given by Equation (1) would be a circle centered at the origin and could sample the nearly continuous $\partial f/\partial v_{\perp} > 0$ that we believe is created by the mirroring of the incident ~keV inverted-V electrons. That such wave modes may exist is shown in Figure 1(a), where an AKR burst appears briefly below the local Ω_e near ~20:49:56 UT, and is consistent with the near 90° polarization observed by FAST. The electron distribution in Figure 1(b) was obtained during this AKR burst, and superimposed on the distribution is a smaller dotted semi-circle which denotes the resonant ellipse given by Equation (1) assuming that $k_{||} \sim 0$ for this burst. As can be seen from the resulting circle, the resonant condition for this AKR emission falls directly on the area where the electron distribution appears to be plateaued. Presumably, the plateaued region of the distribution possessed the largest integrated $\partial f/\partial v_{\perp}$ before the distribution was stabilized, and is where the AKR emissions were able to extract the largest amount of energy for growth.

Conclusion

We have presented several examples of high time resolution contour plots of the electron distributions within the source regions of AKR. The general features of these distributions are (1) a loss cone, (2) a slight positive slope for small pitch angles about the field-aligned direction due to the inverted-V electrons, (3) a broad plateau with a radius close to the primary incident electron acceleration energy and covering pitch angles from near field-aligned all the way back to the loss cone, and (4) occasional enhancements in the distribution at 90° pitch angles which have a strong negative gradient. At present the FAST data resembles the results of computer simulations that examined the contribution of $\partial f/\partial v_{\perp}$ resulting from not only the loss cone but the features produced by the incident inverted-V electrons as well. These results suggest that the source of free energy in the electrons is not limited to the loss cone alone but may encompass a much more extensive region of the distribution. The observation of intense AKR in the source region at frequencies very close to Ω_e and below, as well as the apparent extreme cold plasma density depletion within the source region, is consistent with such a model. Additionally, we find evidence that relativistic modes with a negligible $k_{||}$ would experience optimum growth from the observed electron distributions, since these modes would sample the initial positive gradient of the incident mono-energetic beam most effectively.

Acknowledgements. The authors gratefully acknowledge the entire FAST team of scientists, engineers, and technicians. Thanks to P.L. Pritchett for permission to reproduce the data shown in Figure 3. The research described in this paper was conducted under NASA grant NAG5-3596.

References

Chiu, Y.T., and M. Schulz, Self-consistent particle and parallel electrostatic field distributions in the magnetospheric-ionospheric auroral region, *J. Geophys. Res.*, *83*, 629-642, 1978.

Ergun, R.E., C.W. Carlson, J.P. McFadden, F.S. Mozer, G.T. Delory, W. Peria, C.C. Chaston, M. Temerin, R. Elphic, R. Strangeway, R. Pfaff, C.A. Cattell, D. Klumpar, E. Shelly, W. Peterson, E. Möebius, and L. Kistler, FAST satellite wave observations in the AKR source region, *Geophys. Res. Lett., in press*, 1998.

Gurgiolo, C., and J.L. Burch, Simulation of electron distributions within auroral acceleration regions, *J. Geophys. Res.*, *93*, 3989-4003, 1988.

Louarn, P., A. Roux, H. de Féraudy, D. Le Quéau, M. André, and L. Matson, Trapped electrons as a free energy source for the auroral kilometric radiation, *J. Geophys. Res.*, *95*, 5983-5995, 1990

Menietti, J.D., J.L. Burch, R.M. Winglee, and D.A. Gurnett, DE 1 particle and wave observations in auroral kilometric radiation (AKR) source regions, *J. Geophys. Res.*, *98*, 5865-5879, 1993.

Mizera, P.F., and J.P. Fennell, Signatures of electric fields from high and low altitude particle distributions, *Geophys. Res. Lett., 4*, 311-314, 1977.

Omidi, N., C.S. Wu, and D.A. Gurnett, Generation of auroral kilometric and Z mode radiation by the cyclotron maser mechanism, *J. Geophys. Res.*, *89*, 883-895, 1984.

Pottelette, R., R.A. Treumann, and N. Dubouloz, Generation of auroral kilometric radiation in upper hybrid wave-lower hybrid soliton interaction, *J. Geophys. Res., 97*, 12029-12044, 1992.

Pritchett, P.L., and R.M. Winglee, Generation and propagation of kilometric radiation in the auroral plasma cavity, *J. Geophys. Res., 94*, 129-143, 1989.

Pritchett, P.L., and R.J. Strangeway, A simulation study of kilometric radiation generation along an auroral field line, *J. Geophys. Res., 90*, 9650-9662, 1985.

Shawhan, S.D., and D.A. Gurnett, Polarization measurements of auroral kilometric radiation by dynamics explorer-I, *Geophys. Res. Lett.*, *9*, 913-916, 1982.

Strangeway, R.J., L. Kepko, R.C. Elphic, C.W. Carlson, R.E. Ergun, J.P. McFadden, W.J. Peria, G.T. Delory, C.C. Chaston, M. Temerin, C.A. Cattell, E. Möebius, L.M. Kistler, D.M. Klumpar, W.K. Peterson, E.G. Shelley, and R.F. Pfaff, FAST observations of VLF waves in the auroral zone: Evidence of very low plasma densities, *Geophys. Res. Lett., in press*, 1998.

Strangeway, R.J., On the applicability of relativistic dispersion to auroral zone electron distributions, *J. Geophys. Res.*, *91*, 3152-3166, 1986.

Strangeway, R.J., Wave dispersion and ray propagation in a weakly relativistic electron plasma: Implications for the generation of auroral kilometric radiation, *J. Geophys. Res.*,*90*, 9675-9687, 1985.

Ungstrup, E., A. Bahnsen, H.K. Wong, M. André, and L. Matson, Energy source and generation mechanism for auroral kilometric radiation, *J. Geophys. Res.*,*95*, 5973-5981, 1990.

Winglee, R.M., and P.L. Pritchett, The generation of low-frequency electrostatic waves in association with auroral kilometric radiation, *J. Geophys. Res.*,91, 13531-13541, 1986.

Wu, C.S., and L.C. Lee, A theory of terrestrial kilometric radiation, *Astrophys. J., 230*, 621-626, 1979.

C.W. Carlson, C.C. Chaston, G.T. Delory, R.E. Ergun, J.P. McFadden, L. Muschietti, W. Peria, Space Sciences Laboratory, University of California, Berkeley, CA 94720-7450 (e-mail: gdelory@ssl.berkeley.edu)

R. Strangeway, Institute of Geophysical and Planetary Physics, University of California, Los Angeles, CA 90024 (e-mail: strange@igpp.ucla.edu)

(Received: November 21, 1997; Revised: February 6, 1998; Accepted: February 12, 1998